Optical excitation of deep defect levels in insulators within many-body perturbation theory: The *F* center in calcium fluoride

Yuchen Ma* and Michael Rohlfing
Fachbereich Physik, Universität Osnabrück, D-49069 Osnabrück, Germany
(Received 22 January 2008; published 14 March 2008)

As a prototype for defects in insulators, we discuss the optical properties of the *F* center in calcium fluoride (CaF_2), which constitutes a prominent defect of the material. The *F* center of CaF_2 exhibits a defect state deep in the band gap. Its excitation by light (at 3.3 eV excitation energy) is described by *ab initio* many-body perturbation theory (*GW* approximation and the Bethe–Salpeter equation), including electronic exchange, correlation, and electron-hole interaction effects. The excitation causes strong relaxation of the defect geometry, leading to significant broadening of the optical spectrum by 0.5 eV and to a large Stokes shift of 1.5 eV.

DOI: 10.1103/PhysRevB.77.115118 PACS number(s): 71.35.Cc, 31.50.Df, 61.72.J−, 71.20.−b

I. INTRODUCTION

Calcium fluoride (CaF_2) is an important material for optical applications in the ultraviolet spectral region because of its wide band gap of about 12 eV, its perfect optical isotropy, and its mechanical properties. CaF_2 is used as lens material for deep-ultraviolet (193 nm) and vacuum-ultraviolet microlithographies. Applications at high intensities can be severely hindered by intrinsic defects,[1] among which the *F* center (i.e., a fluorine vacancy) constitutes a common point defect. A systematic understanding and characterization of such defects is of high importance for the further improvement of the material.

Optical excitations of point defects in insulators are often schematically described as transitions between strongly localized deep electronic levels. A quantitative analysis of such transitions, however, is a complicated issue for various reasons. First, it is not clear in many cases if the electronic states are localized or not, even in wide-gap materials such as CaF_2. Often, as in the present case, one of the involved single-particle states is localized (here, the hole state), while the other one is rather delocalized (here, the electron). Second, electronic levels and the optical transitions between them are strongly influenced by electronic many-body effects such as exchange, correlation, dielectric screening, and electron-hole interaction. Third, significant coupling between the excitation and the geometric structure of the defect occurs, causing excited-state relaxation, spectral broadening, and the Stokes shifts.[2] All of these issues must be taken into account on equal footing to achieve the accuracy necessary for quantitative analysis and reliable interpretation of experimental data.

Here, we present a comprehensive analysis of the structural, electronic, and optical properties of the *F* center in CaF_2 by means of state-of-the-art *ab initio* electronic structure approaches. Owing to the complex inter-relation between geometric and electronic degrees of freedom, a combination of density-functional theory (DFT) and *ab initio* many-body perturbation theory (MBPT) is required to deal with all physical mechanisms on equal footing. Within MBPT, electronic exchange and correlation effects are included in the electron self-energy operator in terms of Hedin's *GW* approximation (GWA),[3] accompanied by solving the Bethe–Salpeter equation (BSE) of correlated electron-hole excitations.[4,5] This *GW*+BSE approach has become a standard procedure for optical excitations of many systems[4,6–8] including defects, e.g., in LiCl.[9,10] *GW*+BSE allowed us to investigate the optical spectrum of the CaF_2 bulk crystal.[11] Here, we extend our approach to address an important point defect of the material. In particular, we investigate the coupling of the excited states to the geometric structure of the defect and evaluate the resulting optical line shape and Stokes shift.

The *F* center (shown in Fig. 1) consists of a fluorine vacancy (in the center of the figure), which is surrounded by four nearest-neighbor calcium atoms and six second-nearest-neighbor fluorine atoms. Under normal conditions, the *F* center is charge neutral, i.e., the missing fluorine atom has been removed as a neutral F^0, and the vacancy hosts one unpaired electron (see below). The ground state of the *F* center in CaF_2 is spin doublet. The electronic structure is thus quite similar to the original configuration, in which the site was occupied by a negatively charged F^- anion. Concomitantly, the geometry is also very close to the ideal configuration,[12] just showing some radial relaxation of the neighboring atoms. Within DFT, the first and second nearest neighboring atoms observe only small relaxation (<0.04 Å) from their ideal positions (see Table I).

II. THEORY AND METHOD

The DFT calculations are performed using the SIESTA code,[13] employing the local spin-density approximation

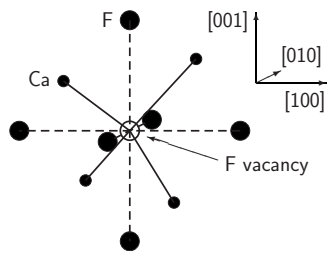

FIG. 1. Structure of the *F* center (fluorine vacancy, indicated as ○) surrounded by four nearest-neighbor Ca atoms (small circles) and six second-nearest-neighbor fluorine atoms (big circles).

TABLE I. Structural data of the F vacancy. The table shows the radial distances of nearest-neighbor Ca atoms and second-nearest-neighbor F atoms from the vacancy. The relaxed structure is obtained from DFT geometry optimization, while the excited-state relaxed structure results from constrained DFT (CDFT) and MBPT geometry optimization (see text).

	$d_{\text{vac-Ca}}$ (Å)	$d_{\text{vac-F}}$ (Å)
Ideal	2.37	2.73
Relaxed (DFT)	2.39	2.70
Excited (CDFT)	2.47	2.58
Excited (MBPT)	2.48	2.56

(LSDA) and norm-conserving Troullier–Martins pseudopotentials. The SIESTA basis set, including that of the ghost atom at the vacancy site, is double ζ plus a single shell of polarization function. In all our calculations [DFT, constrained density-functional theory (CDFT), and GW+BSE], the Ca 3s and 3p semicore electrons are included as valence electrons.[11] We employ a supercell of $2\times2\times2$ primitive fcc unit cells, containing 23 atoms (8 Ca and 15 F atoms). A $3\times3\times3$ supercell yields nearly the same DFT results, indicating that the defect structure is, in fact, of strongly localized nature. All structural optimizations are carried out at the theoretical lattice constant of 5.343 Å (cf. Ref. 12). The obtained structural data are then rescaled to the experimental lattice constant of 5.463 Å, at which the calculations of the excitations take place. The data shown in Table I include this rescaling and should therefore directly refer to the real system.

Subsequent band-structure and optical-spectrum calculations are performed within MBPT (cf. Ref. 11) using the $2\times2\times2$ supercell. All empty-state summations within MBPT employ 315 empty bands, corresponding to 20 empty bands for nonspin-polarized bulk CaF_2.[11] The reciprocal-space summations employ 32 **k** points for the random-phase approximation dielectric matrix, 4 **k** points for the self-energy operator, and 32 **k** points for the representation of optical excitations, which correspond to 256, 32, and 256 **k** points for bulk CaF_2. These specifications (empty-state summation and **k** points sampling) yield excitation energies converged to about 0.1 eV.

III. RESULTS AND DISCUSSIONS

The LSDA and quasiparticle band structures of the defect system are shown in Fig. 2. For each spin channel, LSDA yields a deep level at 5.5–7 eV energy (labeled 1s), accompanied by four additional defect levels at 8–8.5 eV (labeled 2s and 2p). We take the 1$s\uparrow$ state as occupied by the unpaired electron of the F center. The dispersion of the 1s band of about 0.5 eV is caused by the interaction with the F centers in the adjacent supercells. A simple tight-binding analysis results in LSDA on site energies of 6.0 and 6.9 eV for 1$s\uparrow$ and 1$s\downarrow$, respectively. Within GWA, we obtain 7.4 and 11.4 eV for 1$s\uparrow$ and 1$s\downarrow$, i.e., the state observes a significant

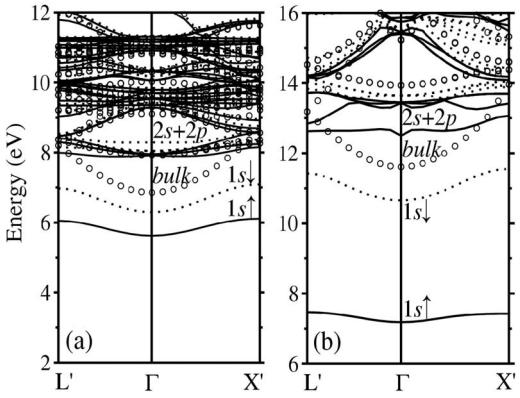

FIG. 2. Band structure of the F center in CaF_2 within (a) LSDA and (b) GWA calculated for a $2\times2\times2$ unit cell. Energies are given relative to the bulk valence band maximum. Solid (dotted) lines indicate the spin-up (down) states. For illustration, the circles indicate the backfolded CaF_2 bulk band structure.

on site interaction of U=4.0 eV.[14] The s-like wave function of this state is basically identical to the hole distribution shown in Fig. 3(d). More than 70% of the unpaired electron is localized inside the vacancy.[12]

The labeling of the defect states as 1s, 2s, etc., suggests a Rydberg-like series of gap states,[15] as is commonly assumed for such defects. Except for 1s, however, the states become resonant with the CaF_2 conduction bands,[2,9,15,16] which are

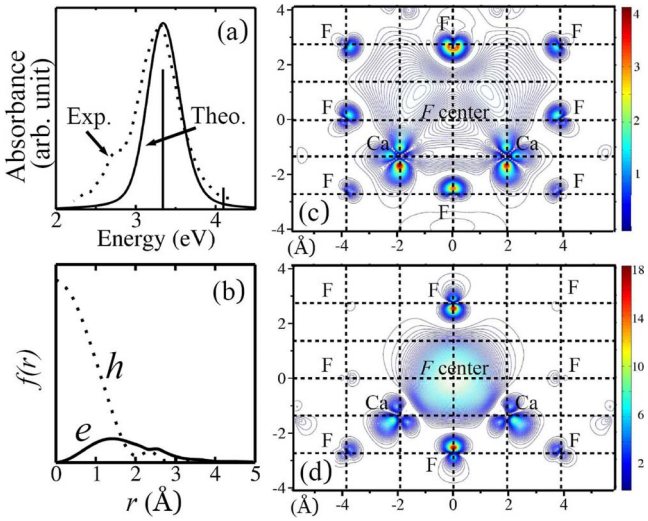

FIG. 3. (Color online) (a) Absorption spectrum of the F center in CaF_2 from MBPT (solid curve) and experiment (dotted curve, from Ref. 17). In the calculation, spectral broadening results from the Franck–Condon factors of the geometric relaxation (see text). The vertical lines indicate the position of the lowest active excitons at 3.3 and 4.2 eV excitation energies, respectively. [(b)–(d)] Spatial distribution of the electron relative to the hole (at the vacancy center) and that of the hole relative to the electron (at the four nearest-neighbor Ca atoms), respectively, for the exciton at 3.3 eV excitation energy. Panel (b) shows the distributions as radial probability functions (normalized such that $4\pi\int_0^\infty f(r)r^2dr=1$). Panels (c) and (d) show the electron and the hole, respectively, in the (110) plane through the vacancy. The atoms are located at the grid points indicated by element symbols.

included in Fig. 2 as circles (as obtained from an independent bulk calculation). Concomitantly, these states are not localized at the defect site but spread out over the entire supercell. Therefore, one cannot expect that a simple $s \rightarrow p$ band-to-band transition can be responsible for the optical excitation of the F center. Instead, local excitations are obtained as coherent superposition of the spatially extended interband transitions (see below).

Within MBPT, optical transitions result from the Bethe–Salpeter equation, taking into account band-structure energies and electron-hole interaction between occupied and empty states. Low-energy transitions of the F center are formed from the localized $1s\uparrow$ defect state and the delocalized unoccupied spin-up states. From those excitations, the optical absorption spectrum is obtained, as shown in Fig. 3(a). Without electron-hole interaction, the absorption spectrum of the noncoupled interband transitions (from the $1s\uparrow$ defect state to the low-lying empty spin-up states) starts at an excitation energy of 5.5 eV. Due to the electron-hole interaction, bound excitons are formed. The most important state is the exciton at 3.3 eV excitation energy, which exhibits excitonic binding of 1.7 eV (stronger than the binding energy of 0.9 eV of the bulk exciton). This exciton occurs as a threefold degenerate state[18] and exhibits p-like symmetry (see below). It is thus tempting to consider this excitation as a $s \rightarrow p$ transition, as it would commonly be expected from a Rydberg series of defect states. In the present situation, however, the formation of the state is more complicated (see below). As a consequence of strong exciton-phonon coupling, the exciton observes significant spectral broadening. Our geometry-dependent BSE data of the exciton (see the discussion below) allow us to evaluate its line shape, which is shown by the solid curve in Fig. 3(a), in very gratifying agreement with the experimental data indicated by the dotted curve.[17] We find additional exciton states above 3.3 eV excitation energy. Most of them are given by optically inactive charge-transfer states between the defect and neighboring atoms. Two optically allowed transitions are found at 4.2 and 4.9 eV excitation energies, but their dipole strengths are much smaller than that of the 3.3 eV transition.

Detailed information about the spatial properties of the exciton is obtained from its two-particle wave function. Figure 3 shows the resulting distribution of the excited electron [panel (c)] and of the hole [panel (d)] in the (110) plane cutting through the defect. Panel (b) shows the same physical quantities as radial probability distributions. Figure 3 illustrates that the simple concept of the exciton as an $s \rightarrow p$ transition is qualitatively correct. The quantitative details, however, are very complex. (i) Both the hole and the electron are localized at the defect (within about 2 Å for the hole and 4 Å for the electron), but they also have significant amplitude on the neighboring atoms. (ii) The hole is localized at the defect because it is a deep defect state. The localization of the electron, on the other hand, is caused by the attraction to the hole (resulting from the BSE), while the electronic single-particle states on their own are all delocalized (see the discussion above).

The excitation causes significant changes in the electronic charge distribution because the excited electron is more extended than the hole (see Fig. 3). This is due to the delocalization of the single-particle states of which the electron is composed and due to the p-like symmetry of the electron enforcing zero amplitude in the vacancy center. Consequently, the vacancy becomes positively charged in its center, surrounded by a negative charge density extending several angstroms. While the entire defect still appears charge neutral at larger distance, significant electrostatic forces on the ions (Ca^{2+} and F^-) arise within a radius of about 3–4 Å. Consequently, the nearest-neighbor Ca^{2+} cations are repelled from the defect site by about 0.09 Å, while the second-nearest-neighbor F^- anions are attracted by 0.14 Å (see Table I). The associated changes in total energy have dramatic consequences for the line shape of the excitation spectrum (see below).

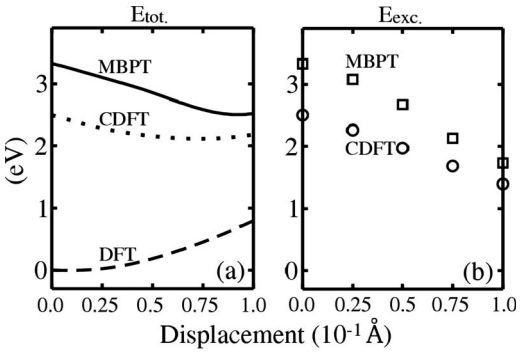

FIG. 4. (a) Total energies of the ground state (DFT, dashed line) and those of the excited state within MBPT (solid line) and CDFT (dotted line) along the relaxation path resulting from CDFT. (b) Excitation energies calculated within MBPT (□) and CDFT (○) along the relaxation path. The abscissa in both panels is the displacement of the nearest-neighbor Ca^{2+} cations in the radial direction from their ground-state equilibrium positions.

In general, the detailed analysis of such relaxation requires to optimize the geometric structure in the excited state based on forces from MBPT.[19,20] However, CaF_2 is a quite complex system[11] and calculations of excited-state forces within MBPT are numerically demanding. Therefore, we treat the geometry relaxation in the excited state by CDFT, in which the highest valence state ($1s\uparrow$) is depopulated and the lowest spin-↑ conduction state is populated instead. Such procedure is well suited for excited states that are distributed over many atoms, causing only small changes of the electronic charge density at each atom.[21] In the present case, however, the excited charge has significantly larger amplitude in the vicinity of the defect, which may make CDFT questionable. In addition, it is not clear *a priori* if CDFT yields the correct density distribution of the excited electron, which is given by a linear combination of many wave functions and is thus not fully described by CDFT.

To check the reliability of the CDFT and of the obtained relaxation, we have carried out additional MBPT calculations for the changed geometries as obtained from CDFT. We assume that the *direction* of the geometry change is given correctly by CDFT, with direction meaning a one-dimensional line $\mathbf{s}$ in the multidimensional configuration space of the coordinates of all atoms around the defect, i.e., $\mathbf{R}=\mathbf{R}_0+\lambda\cdot\mathbf{s}$. Figure 4 shows the resulting total energies [panel (a)] and

excitation energies [panel (b)] along direction **s** as a function of the displacement of the nearest-neighbor Ca^{2+} cations from their ground-state equilibrium positions. The results of CDFT and MBPT are in very gratifying agreement with each other, indicating that CDFT is a suitable procedure for the excited-state relaxation, even for a strongly localized excitation with large changes of the charge density. Nonetheless, three differences between CDFT and MBPT should be pointed out: (i) MBPT yields a steeper slope of the excitation energies than CDFT, (ii) MBPT reaches the excited-state total-energy minimum somewhat later than CDFT, indicating larger excited-state structural relaxation, and (iii) the excitation energies given by MBPT are significantly larger (and much more realistic) than those of CDFT.

The data shown in Fig. 4 allow us to address the optical excitation process in more detail. The total-energy curves together with the relaxation pattern allow us to attribute vibrational frequencies of 40 meV to the ground state and 35 meV to the excited state.[22] Assuming that at zero temperature the system is in the $(\nu=0)$ vibrational level of the ground state, we calculate the Franck–Condon factors for the transitions into the vibrational levels of the excited state. After including additional artificial broadening of 70 meV, the lowest-energy exciton yields the optical excitation spectrum shown in Fig. 3(a), exhibiting a line shape, in good agreement with the experimental data,[17] with a spectral width (full width at half maximum) of 0.5 eV. Furthermore, the total-energy data of Fig. 4 yield a strong Stokes shift of 1.5 eV (i.e., difference between the vertical excitation energies at the ground-state and excited-state equilibria), suggesting that light emission would take place at an energy of 1.8 eV. In fact, laser irradiated CaF_2 crystals show an emission band at 1.7 eV,[1] which could thus be assigned to the *F* center.

IV. SUMMARY

In summary, we have investigated the optical excitation of the *F* center in CaF_2 using a combination of constrained DFT and *ab initio* many-body perturbation theory. Our calculations predict the absorption band and the emission band of the *F* center at 3.3 and 1.8 eV, respectively, in good agreement with experiments. The exciton of the absorption band is strongly localized around the vacancy within 4.0 Å, inducing prominent lattice distortion around the defect. Our results demonstrate that constrained DFT can predict reliable geometric relaxation for localized excitons in ionic insulators. Quantitative results for the corresponding excitation energies and optical spectra, however, require a more elaborate approach such as *ab initio* many-body perturbation theory.

ACKNOWLEDGMENTS

This work has been supported by the Deutsche Forschungsgemeinschaft (Bonn, Germany) under Grant No. Ro 1318/4-3.

*yuma@uos.de

[1] C. Mühlig, W. Triebel, G. Töpfer, J. Bergman, S. Brückner, C. Chojetzki, and R. Martin, Proc. SPIE **5188**, 123 (2003).
[2] W. B. Fowler, in *Physics of Color Centers*, edited by W. B. Fowler (Academic, New York, 1968).
[3] L. Hedin and S. Lundqvist, in *Solid State Physics: Advances in Research and Application*, edited by F. Seitz, D. Turnbull, and H. Ehrenreich (Academic, New York, 1969), Vol. 23, p. 1.
[4] M. Rohlfing and S. G. Louie, Phys. Rev. B **62**, 4927 (2000).
[5] G. Onida, L. Reining, and A. Rubio, Rev. Mod. Phys. **74**, 601 (2002).
[6] E. L. Shirley, Phys. Rev. Lett. **80**, 794 (1998).
[7] L. X. Benedict, E. L. Shirley, and R. B. Bohn, Phys. Rev. Lett. **80**, 4514 (1998).
[8] S. Albrecht, L. Reining, R. Del Sole, and G. Onida, Phys. Rev. Lett. **80**, 4510 (1998).
[9] M. P. Surh, H. Chacham, and S. G. Louie, Phys. Rev. B **51**, 7464 (1995).
[10] M. L. Tiago and J. R. Chelikowsky, Phys. Rev. B **73**, 205334 (2006).
[11] Y. C. Ma and M. Rohlfing, Phys. Rev. B **75**, 205114 (2007).
[12] H. Shi, R. I. Eglitis, and G. Borstel, Phys. Rev. B **72**, 045109 (2005).
[13] J. M. Soler, E. Artacho, J. D. Gale, A. García, J. Junquera, P. Ordejón, and D. Sánchez-Portal, J. Phys.: Condens. Matter **14**, 2745 (2002).
[14] M. Rohlfing and J. Pollmann, Phys. Rev. Lett. **84**, 135 (2000).
[15] N. F. Mott and R. W. Gurney, *Electronic Processes in Ionic Crystals* (Dover, New York, 1964), pp. 80 and 114.
[16] B. M. Klein, W. E. Pickett, L. L. Boyer, and R. Zeller, Phys. Rev. B **35**, 5802 (1987).
[17] D. A. Patterson and R. G. Fuller, Phys. Rev. Lett. **18**, 1123 (1967).
[18] In the present calculation, we observe twofold degeneracy, while the third exciton is split off by the electron-hole exchange interaction. This is a consequence of our finite supercell and would vanish for increasing cell size.
[19] S. Ismail-Beigi and S. G. Louie, Phys. Rev. Lett. **90**, 076401 (2003).
[20] S. Ismail-Beigi and S. G. Louie, Phys. Rev. Lett. **95**, 156401 (2005).
[21] E. Artacho, M. Rohlfing, M. Côté, P. D. Haynes, R. J. Needs, and C. Molteni, Phys. Rev. Lett. **93**, 116401 (2004).
[22] G. J. Exarhos, J. Phys. Chem. **86**, 4020 (1982).